Local Stress Differential for Particulate Fracture in AA2024/Titanium Carbide Nanoparticulate Metal Matrix Composites

A. Chennakesava Reddy

Assistant Professor, Department of Mechanical Engineering, MJ College of Engineering and Technology, Hyderabad, India
dr_acreddy@yahoo.com

Abstract: *Hexagonal array unit cell/2-D elliptical particulate RVE models were used to evaluate interface debonding and particulate fracture using two-dimensional finite element methods. The particulate metal matrix composites are titanium carbide/AA2024 alloy at different volume fractions of titanium carbide. The titanium carbide particulate was ruptured in the composites having 30%TiC due to large variation of local stress across the particulate.*

Keywords: AA2024*, titanium carbide, elliptical particle, RVE model, finite element analysis, debonding, particulate fracture.*

1. INTRODUCTION

Metal composite materials (MMCs) have found application in many areas of daily life for quite some time. These innovative materials open up unlimited possibilities for modern material science and development; the characteristics of MMCs can be designed into the material, custom-made, dependent on the application. From this potential, metal matrix composites fulfill all the desired conceptions of the designer. The characteristics of metal matrix composite materials are determined by their microstructure and internal interfaces. Chemical interactions and reactions between the matrix and the reinforcement component determine the interface adhesion, modify the characteristics of the composite components and affect the mechanical characteristics significantly. Fracture of reinforcement particles either during processing or during subsequent mechanical loading has been observed experimentally in discontinuously particulate-reinforced metal matrix composites [1, 2]. Finite element analyses are also used to study the overall elastic properties of two-phase discontinuously particulate-reinforced metal matrix composites (DMMCs) as a function of the shape, concentration, and spatial distribution of the reinforcement particles [3-13].

The objective of this paper is to predict debonding in AA2024 alloy/titanium carbide particulate metal matrix composites. Representative volume elements (RVEs) models were modeled using finite element method. The RVEs were taken from the periodic 2-D elliptical particulates in a hexagonal array distribution.

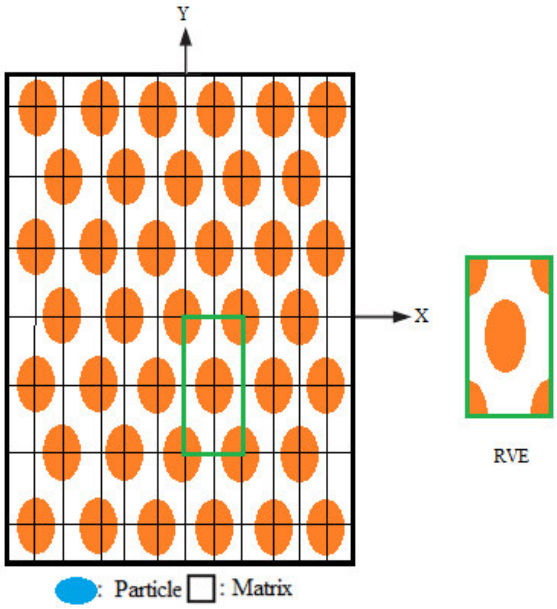

Figure 1: The RVE model: (a) particle distribution and (b) RVE scheme.

2. MATERIALS AND METHODS

The AA2024 alloy/titanium carbide nanoparticulate metal matrix composites were used in the present work with 10%, 20%, and 30% volume fractions of titanium carbide. The periodic model for the representative volume element (RVE) scheme as shown in figure 1 was used to analyze the composites with ANSYS software code. The RVE scheme was constructed from 2-D elliptical particulates in a hexagonal array particulate distribution. The perfect adhesion was assumed between titanium carbide particle and AA2034 alloy matrix. PLANE183 element was used for the matrix and the nanoparticle. The interface between particle and matrix was modeled using CONTACT -172 elements.

If particle fracture occurs when the stress in the particle reaches its ultimate tensile strength, $\sigma_{p,uts}$, then setting the boundary condition at

$$\sigma_p = \sigma_{p,\ uts} \tag{1}$$

and substituting into Eq.(1) gives a relationship between the strength of the particle and the interfacial shear stress such that if

$$\sigma_{P,uts} < \frac{2\tau}{n} \tag{2}$$

Then the particle will fracture. Similarly if interfacial debonding/yielding is considered to occur when the interfacial shear stress reaches its shear strength

$$\tau = \tau_{max} \tag{3}$$

Then by substituting Eq. (5) into Eq.(1) a boundary condition for particle/matrix interfacial fracture can be established whereby,

$$\tau_{max} < \frac{n\sigma_p}{2} \tag{4}$$

This approach suggests that the outcome of a matrix crack impinging on an embedded particle depends on the balance between the particle strength and the shear strength of the interface.

A linear stress–strain relation at the macro level can be formulated as follows:

$$\bar{\sigma} = \overline{C}\bar{\varepsilon} \tag{5}$$

where $\bar{\sigma}$ is macro stress, and $\bar{\varepsilon}$ represents macro total strain and $\overline{C}$ and is macro stiffness matrix.

For plane strain conditions, the macro stress- macro strain relation is as follows:

$$\begin{Bmatrix} \overline{\sigma_x} \\ \overline{\sigma_y} \\ \overline{\tau_{xy}} \end{Bmatrix} = \begin{bmatrix} \overline{C_{11}} & \overline{C_{12}} & 0 \\ \overline{C_{21}} & \overline{C_{22}} & 0 \\ 0 & 0 & \overline{C_{33}} \end{bmatrix} \times \begin{Bmatrix} \overline{\varepsilon_x} \\ \overline{\varepsilon_y} \\ \overline{\gamma_{xy}} \end{Bmatrix} \tag{6}$$

The interfacial tractions can be obtained by transforming the micro stresses at the interface as given in Eq. (3):

$$t = \begin{Bmatrix} t_z \\ t_n \\ t_t \end{Bmatrix} = T\sigma \tag{7}$$

where, $T = \begin{bmatrix} 0 & 0 & 0 \\ cos^2\theta & sin^2\theta & 2sin\theta cos\theta \\ -sin\theta cos\theta & sin\theta cos\theta & cos^2\theta - sin^2\theta \end{bmatrix}$

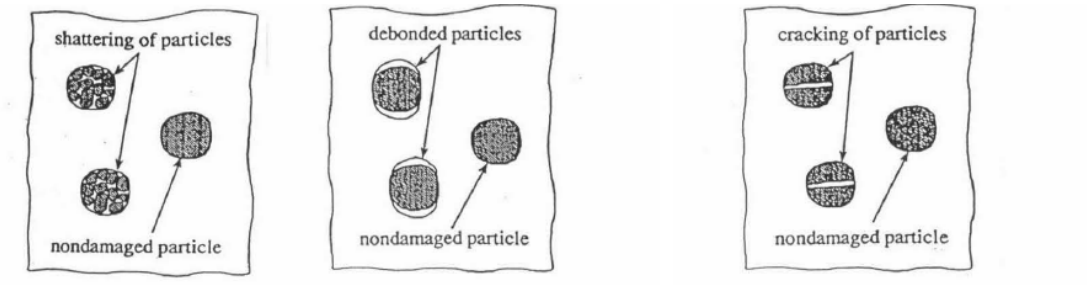

(a) shattered particles producing complete voids. (b) particles with the debonded interface producing debonded particles. (c) cracked particles producing penny-shaped cracks within the particles.

Figure 2: Schematic of three particle damage modes in metal matrix composites reinforced with spherical particles.

For the three cases of the shattering of particles producing complete voids, debonded particles, and particles containing single penny-shaped cracks (figure 2), their results can be summarized as

$$\frac{E_c}{E_m} = \frac{1}{1+\eta_p(1-V_d)V_p+\eta_d V_d V_o} \quad (8)$$

Where E_c and E_m are elastic moduli of the composite and matrix, respectively, V_p is the volume fraction of total particle reinforcements, V_d is the volume fraction of damaged particles in terms of total particles, and η_p and η_d are function of V_p and V_d and elastic moduli of matrix and reinforcements [15].

3. RESULTS AND DISCUSSION

The effect of titanium carbide content on the elastic moduli, E_x, E_y and G_{xy} is shown figure 3a. The tensile elastic modulus increased with the increase of titanium carbide content in the composites. The compressive and shear moduli of AA2024 alloy 20%TiC composites were lower than those of AA2024 alloy 10%TiC and AA2024 alloy 30%TiC composites. The major Poisson's ratio decreased with increase of volume fraction of TiC (figure 3b).

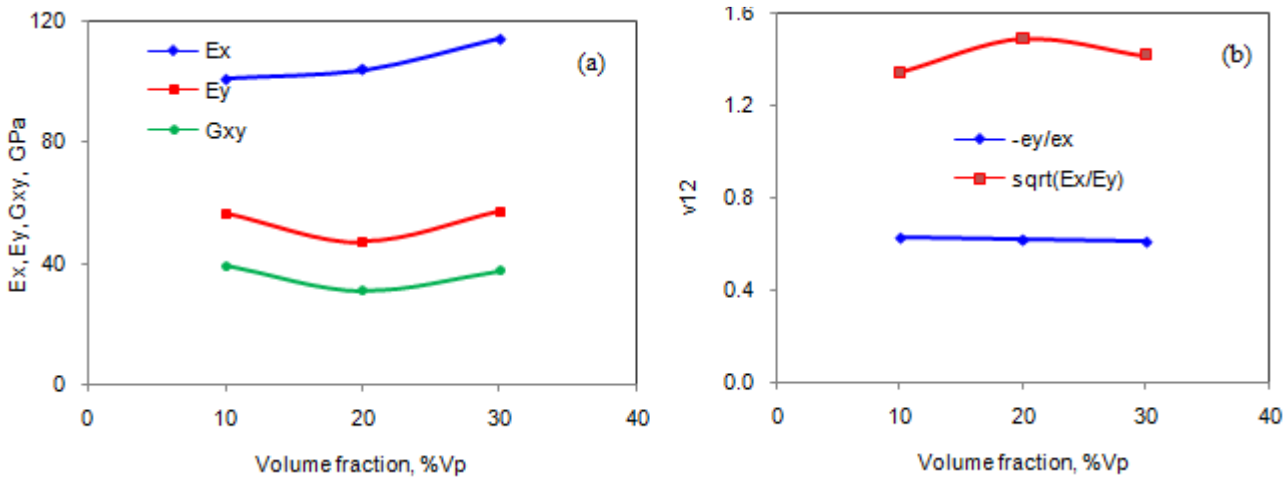

Figure 3: Effect of volume fraction on effective material properties.

The particulate fracture was occurred in the composites having 30% TiC particulates as shown in figure 4a. The TiC particulate fracture was noticed as the condition $\sigma_p \leq 2\tau/n$ is satisfied. The condition, $\tau_{max} < n\sigma_p/2$ is satisfied for the occurrence of debonding in the composites having 10% and 20%TiC particulates (figure 4b). The normal and tangential tractions developed at the interface increased with the increase of TiC content in the composites (figure 5).

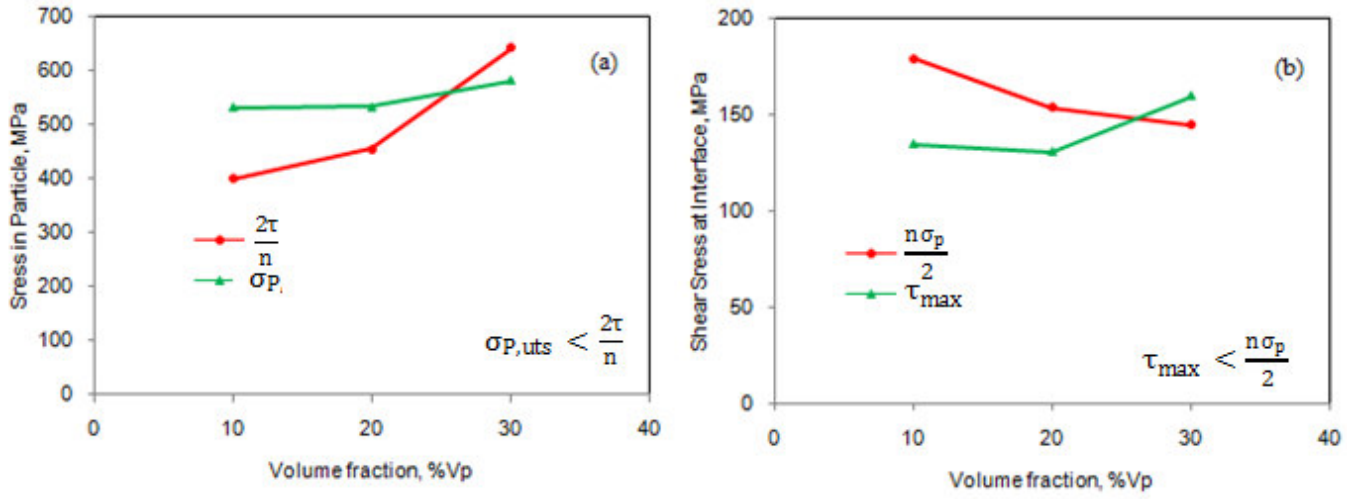

Figure 4: Fracture criteria of: (a) particulate fracture and (b) interface debonding.

In TiC particulates, the stress intensities were, respectively, 458.13 MPa, 464.96 MPa and 462. 74 MPa in the composites having 10% TiC, 20%TiC and 30% TiC (figure 6). The stress variation is nil across the particle in the composites having 10% TiC. The stress variation is 45 MPa across the particle in the composites having 20% TiC. The stress variation is 52 MPa across the particle in the composites having 30% TiC. High differential stress across TiC particle is attributable to fracture of TiC Particulate in the composites having 30% TiC.

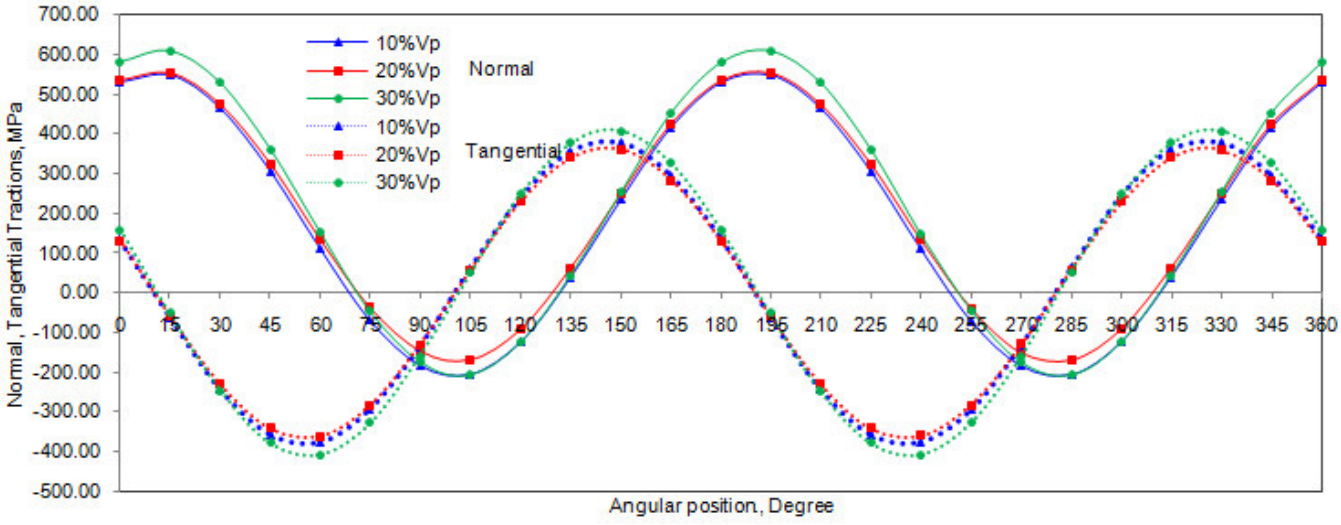

Figure 5: Normal and tangential interactions.

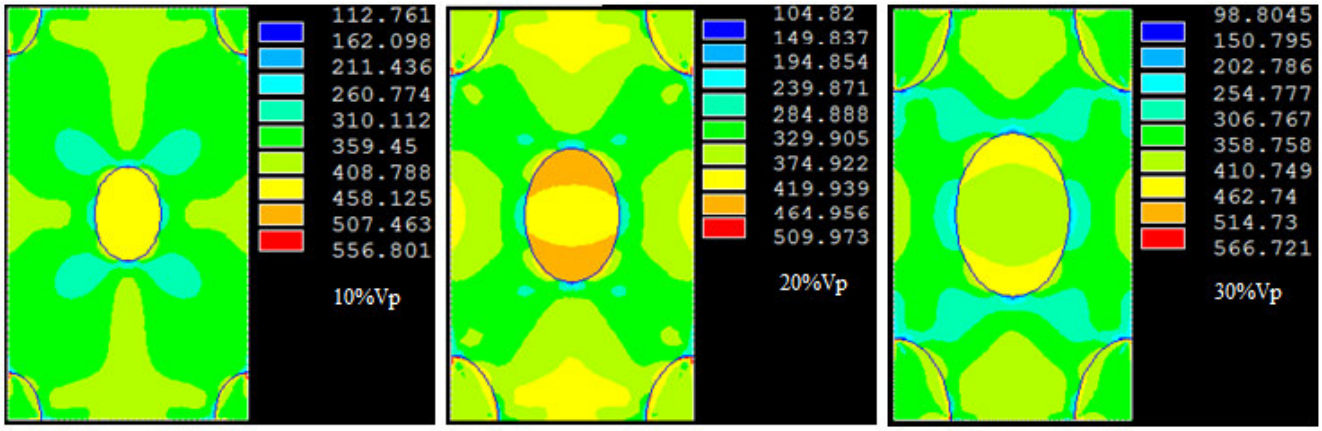

Figure 6: Results obtained from finite element analysis: stress intensities.

4. CONCLUSION

The interface debonding took place in the composites having 10% and 20% volume fractions of TiC. The Particulate fracture was observed in the composites having 30% TiC. The particulate fracture was due to large variation of local stress across TiC particulates.

REFERENCES

1. T. Christman, K. Heady and T. Vreeland, Jr., Consolidation of Ti-SiC particle-reinforced metal-matrix composites, Scripta Metal/. Mater., 25, 1991, pp. 631-6.
2. D.J. Lloyd, Aspects of fracture in particulate reinforced metal matrix composites, Acta Metal/. Mater., 39, 1991, pp. 59-71.
3. S. Sundara Rajan and A. Chennakesava Reddy, Assessment of Tensile Behavior of Boron Carbide/AA2024 Alloy Metal Matrix Composites, 1st International Conference on Composite Materials and Characterization, Bangalore, March 1997, pp.160-163.
4. P. Martin Jebaraj and A. Chennakesava Reddy, Prediction of Micro-stresses and interfacial Tractions in Boron Carbide/AA6061 Alloy Metal Matrix Composites, 1st International Conference on Composite Materials and Characterization, Bangalore, March 1997, pp. 183-185.

5. B. Kotiveera Chari and A. Chennakesava Reddy, Computation of Micro-stresses and interfacial Tractions in Boron Carbide/AA7020 Alloy Metal Matrix Composites, 1st International Conference on Composite Materials and Characterization, Bangalore, March 1997, pp. 186-188.
6. P. Martin Jebaraj, A. Chennakesava Reddy, Effect of Interfacial Debonding on Stiffness of Titanium Boride/AA5050 Alloy Metal Matrix Composites, 1st National Conference on Modern Materials and Manufacturing , Pune, 19-20 December, 1997.
7. S. Sundara Rajan, A. Chennakesava Reddy, Micromechanical modeling of Titanium Boride/AA7020 Alloy Metal Matrix Composites in Finite Element Analysis using RVE Model, 1st National Conference on Modern Materials and Manufacturing, Pune, 19-20 December, 1997.
8. P. Martin Jebaraj, A. Chennakesava Reddy, Effect of Interfacial Tractions of Rectangular Titanium Boride Particulate/AA8090 Alloy Metal Matrix Composites , 1st National Conference on Modern Materials and Manufacturing, Pune, 19-20 December, 1997.
9. S. Sundara Rajan, A. Chennakesava Reddy, Cohesive Zone interfacial debonding of Silicon Nitride/AA1100 Alloy Metal Matrix Composites Using Finite Element Analysis , 1st National Conference on Modern Materials and Manufacturing, Pune, 19-20 December, 1997.
10. S. Sundara Rajan, A. Chennakesava Reddy, Simulation of Micromechanics for interfacial debonding in Silicon Nitride/AA2024 Alloy Metal Matrix Composites , 1st National Conference on Modern Materials and Manufacturing , Pune, 19-20 December, 1997.
11. P. Martin Jebaraj, A. Chennakesava Reddy, Finite Element Analysis for Assessment of Dislocation and Debonding Events in Silicon Nitride/AA3003 Alloy Metal Matrix Composites, 1st National Conference on Modern Materials and Manufacturing, Pune, 19-20 December, 1997.
12. A. Chennakesava Reddy, Evaluation of Debonding and Dislocation Occurrences in Rhombus Silicon Nitride Particulate/AA4015 Alloy Metal Matrix Composites, 1st National Conference on Modern Materials and Manufacturing, Pune, India, 19-20 December, 278-282, 1997.
13. T. Mochida, M. Taya and M. Obata, Effect of damaged particles on the stiffness of a particle/metal matrix composite, JSME Inti. J., Series I, 34, 1991, pp. 187-93.